

Accurate Determination of Acceptor Densities and Acceptor Levels in Undoped InGaSb from Temperature Dependence of Hole Concentration

Hideharu MATSUURA*, Kazuhiro NISHIKAWA, Masaharu SEGAWA and Wataru SUSAKI

Department of Electronic Engineering and Computer Science, Osaka Electro-Communication University,
18-8 Hatsu-cho, Neyagawa, Osaka 572-8530, Japan

(Received April 3, 2006; accepted April 19, 2006; published online August 4, 2006)

Without any assumptions regarding residual impurity species and intrinsic defects in an undoped semiconductor, it is experimentally demonstrated that the densities and energy levels of impurities and defects can be precisely determined by a graphical peak analysis method based on Hall-effect measurements, referred to as free-carrier-concentration spectroscopy (FCCS). By FCCS, the number of acceptor species in p-type undoped $\text{In}_{0.2}\text{Ga}_{0.8}\text{Sb}$ epilayers is determined, and the densities and energy levels of these acceptor species are accurately estimated. Two acceptor species, whose acceptor levels are $E_V + 25$ meV and $E_V + 86$ meV, are detected, where E_V is the valence band maximum. The density of the $E_V + 25$ meV acceptor increases with $\text{Sb}_4/(\text{In} + \text{Ga})$ flux beam equivalent pressure (BEP) ratio, whereas the density of the $E_V + 86$ meV acceptor decreases with increasing BEP ratio. These observations are not consistent with the conventional assumption that these acceptor species are V_{Sb}^+ and V_{Sb}^{2+} in GaSb-based semiconductors, where V_{Sb} is the Sb vacancy.

[DOI: 10.1143/JJAP.45.6373]

KEYWORDS: InGaSb, acceptor, Hall-effect measurement, acceptor density, acceptor level, determination of density and energy level, temperature dependence of hole concentration

GaSb-based semiconductors have been regarded as promising materials for the fabrication of near- and mid-infrared laser diodes and photodiodes, which can be used for monitoring the concentrations of gases (CO_2 , CO , NO_x , and SO_x), which cause environmental problems in the atmosphere.¹⁾ In GaSb-based laser diodes, an undoped $\text{In}_x\text{Ga}_{1-x}\text{Sb}$ epilayer, called a well layer, plays an important role in emitting near- and mid-infrared light. This layer has a band gap shallower than that of a cladding layer (e.g., n- or p-type $\text{Al}_x\text{Ga}_{1-x}\text{Sb}$) that injects electrons or holes into the well layer.

Because residual impurities and intrinsic defects in the well layer strongly degrade light-emitting efficiency, it is important to investigate them. Undoped GaSb-based semiconductors usually exhibit a p-type conduction. Using the temperature dependence of hole concentration, $p(T)$, obtained by Hall-effect measurements, the densities and energy levels of residual impurities and intrinsic defects in GaSb-based semiconductors were investigated.^{2–11)} Although the acceptor level and acceptor density are usually determined from the slope and saturation of $\ln p(T) - 1/T$ plots, this analysis cannot be applied to semiconductors with more than one acceptor species and compensated semiconductors. Moreover, it is difficult to obtain reliable values by fitting a curve to the experimental data of $p(T)$, partially because the number (n_{species}) of acceptor species in the semiconductor must be assumed before the analysis and partially because numerous curve-fitting parameters must be simultaneously determined. To reduce the number of curve-fitting parameters, the following assumptions were adopted for undoped GaSb. According to the double-acceptor model where the acceptor can be ionized singly as well as doubly,^{2,3,5,6)} it is assumed that the two acceptor species have the same densities, but different energy levels.

Without any assumptions regarding the acceptor species (e.g., n_{species}), graphical peak analysis methods can accurately determine the densities and energy levels of acceptors. Although Hoffmann and coworkers^{12,13)} proposed a differ-

ential evaluation of $p(T)$, the differential of experimental data causes an increase in observed errors. One of the authors has proposed and tested a precise determination method without the differential evaluation of $p(T)$, referred to as free-carrier-concentration spectroscopy (FCCS),^{14,15)} and has applied FCCS to p-type Si irradiated with high-energy protons or electrons,^{16–18)} SiC,^{19–27)} GaN,²⁸⁾ GaSb,¹⁰⁾ and $\text{Al}_{0.6}\text{Ga}_{0.4}\text{Sb}$.¹¹⁾ Because each peak in the FCCS signal corresponds one-to-one to an impurity or a defect, its density and energy level can be determined accurately from the peak even when n_{species} is unknown. For example, it was difficult to assume n_{species} in undoped GaSb and undoped $\text{Al}_{0.6}\text{Ga}_{0.4}\text{Sb}$.^{10,11)} Moreover, two types of acceptor species were observed in Al-doped 4H-SiC epilayers,²⁵⁾ although only one acceptor species (i.e., Al acceptor) was expected.

By FCCS we determined the densities and energy levels of residual impurities and intrinsic defects in p-type undoped $\text{In}_{0.2}\text{Ga}_{0.8}\text{Sb}$ epilayers grown by molecular beam epitaxy (MBE), and investigated the dependence of the acceptor densities on $\text{Sb}_4/(\text{In} + \text{Ga})$ flux beam equivalent pressure (BEP) ratio during the growth of the epilayers.

Two-micrometer (2- μm)-thick undoped $\text{In}_{0.2}\text{Ga}_{0.8}\text{Sb}$ epilayers were grown on semi-insulating (100) GaAs at 470 °C by water-cooled MBE at three different BEP ratios of 2, 3, and 5. The growth rate was approximately 0.5 $\mu\text{m}/\text{h}$. After each undoped $\text{In}_{0.2}\text{Ga}_{0.8}\text{Sb}$ epilayer was cut into pieces of $7 \times 7 \text{ mm}^2$ size, $p(T)$ was measured by the van der Pauw method in a temperature range from 140 to 300 K at a magnetic field of 1.4 T and a current of 0.1 mA.

Figure 1 shows a set of three $p(T)$ values for undoped $\text{In}_{0.2}\text{Ga}_{0.8}\text{Sb}$ epilayers for the BEP ratios of 2, 3, and 5, denoted by \triangle , \square , and \circ , respectively. The solid lines represent the interpolations of $p(T)$. In the figure, $p(T)$ for the BEP ratio of 2 is the lowest, whereas $p(T)$ for the BEP ratio of 5 is the highest.

There were no straight lines and saturation regions in the $\ln p(T) - 1/T$ plots. Moreover, it was quite difficult to assume n_{species} from the plots. Therefore, it is difficult to analyze $p(T)$ by conventional methods.

The FCCS signal is defined by¹⁰⁾

*E-mail address: matsuura@isc.osakac.ac.jp

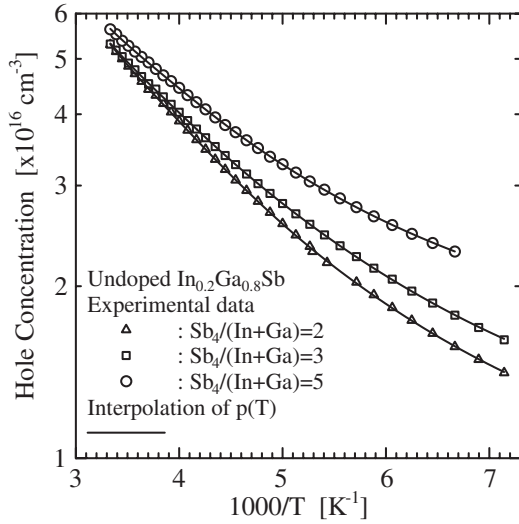


Fig. 1. Temperature dependence of hole concentration in undoped $\text{In}_{0.2}\text{Ga}_{0.8}\text{Sb}$ epilayers grown at different $\text{Sb}_4/(\text{In} + \text{Ga})$ BEP ratios.

$$H(T, E_{\text{ref}}) \equiv \frac{p(T)^2}{(kT)^{5/2}} \exp\left(\frac{E_{\text{ref}}}{kT}\right), \quad (1)$$

where k is the Boltzmann constant and E_{ref} is the parameter that shifts the peak of the FCCS signal within the measurement temperature range. On the other hand, the signal can theoretically be derived as¹⁰⁾

$$H(T, E_{\text{ref}}) = \sum_{i=1}^{n_{\text{species}}} \frac{N_{A_i}}{kT} \exp\left(-\frac{E_{A_i} - E_{\text{ref}}}{kT}\right) I(E_{A_i}) - \frac{N_D N_{V0}}{kT} \exp\left(\frac{E_{\text{ref}} - E_F(T)}{kT}\right), \quad (2)$$

where $I(E_{A_i}) = N_{V0} \exp\{[E_{A_i} - E_F(T)]/kT\} f_{\text{FD}}(E_{A_i})$, N_{A_i} and E_{A_i} are the density and energy level of an i th acceptor species, respectively, $E_F(T)$ is the Fermi level, $f_{\text{FD}}(E_{A_i})$ is the Fermi-Dirac distribution function, N_D is the donor density, N_{V0} is $2(2\pi m_p^*/h^2)^{3/2}$, m_p^* is the hole effective mass, and h is Planck's constant. The Windows application software for FCCS can be freely downloaded at our web site (<http://www.osakac.ac.jp/labs/matsuura/>). This software can also be used by the curve-fitting method or Hoffmann's method.

Figure 2 shows the FCCS signal with E_{ref} of 2.9×10^{-3} eV, calculated using eq. (1) and the interpolation of $p(T)$ for the BEP ratio of 5. In the figure, one peak appears at 265 K, whereas another peak appears at < 150 K. From the peak temperature and the peak value of $3.32 \times 10^{37} \text{ cm}^{-6} \text{ eV}^{-2.5}$, the values of E_{A2} and N_{A2} were determined as $E_V + 86$ meV and $7.3 \times 10^{16} \text{ cm}^{-3}$, respectively.

To investigate another acceptor species, the FCCS signal of $H2(T, E_{\text{ref}})$, in which the influence of the previously determined acceptor species is removed, is calculated using

$$H2(T, E_{\text{ref}}) = \frac{p(T)^2}{(kT)^{5/2}} \exp\left(\frac{E_{\text{ref}}}{kT}\right) - \frac{N_{A2}}{kT} \exp\left(-\frac{E_{A2} - E_{\text{ref}}}{kT}\right) I(E_{A2}), \quad (3)$$

as is clear from eq. (2). The $H2(T, E_{\text{ref}})$ with E_{ref} of -1.4×10^{-2} eV is shown in Fig. 3. Because the peak temperature

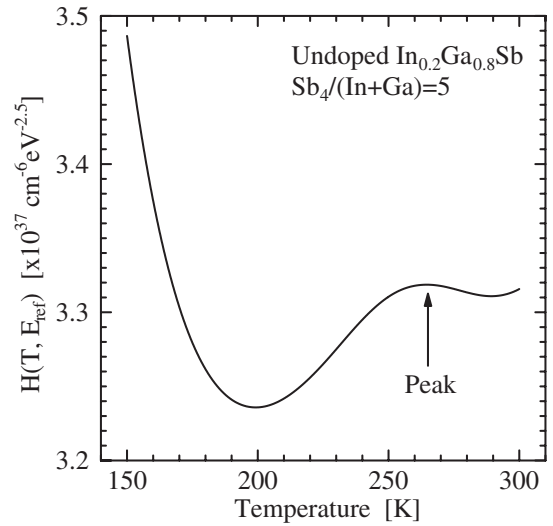


Fig. 2. FCCS signal with E_{ref} of 2.9×10^{-3} eV.

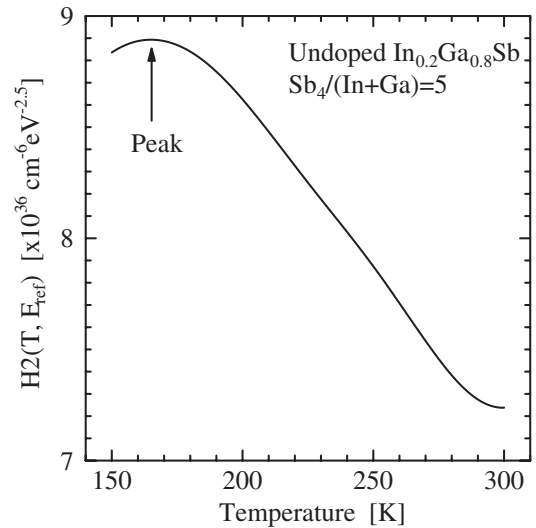


Fig. 3. FCCS signal with E_{ref} of -1.4×10^{-2} eV, in which influence of previously determined acceptor species is removed.

and peak value were 165 K and $8.89 \times 10^{36} \text{ cm}^{-6} \text{ eV}^{-2.5}$, the values of E_{A1} and N_{A1} were determined as $E_V + 25$ meV and $3.1 \times 10^{16} \text{ cm}^{-3}$, respectively.

Although the FCCS signal of $H3(T, E_{\text{ref}})$, in which the influence of two previously determined acceptor species was removed, was calculated, the $H3(T, E_{\text{ref}})$ was nearly zero. Therefore, this epilayer includes two types of acceptor species.

In the same manner as illustrated for the previously mentioned sample, $p(T)$ values for the other samples were analyzed. For all the samples, the values of E_{A1} and E_{A2} were $E_V + 25$ meV and $E_V + 86$ meV, respectively. The values of N_{A1} and N_{A2} are listed in Table I.

Figure 4 shows the experimental $p(T)$ and simulated $p(T)$ (—) with the values shown in Table I. Each $p(T)$ simulation was in good agreement with the corresponding experimental $p(T)$. Therefore, the values obtained by FCCS are reliable.

During the growth of $\text{In}_{0.2}\text{Ga}_{0.8}\text{Sb}$ epilayers at 470°C by MBE, Sb was more apt to be evaporated from the epilayer

Table I. Results determined by FCCS.

BEP ratio	2	3	5
E_{A1} (meV)	$E_V + 25$	$E_V + 25$	$E_V + 25$
N_{A1} ($\times 10^{16}$ cm $^{-3}$)	1.7	2.2	3.1
E_{A2} (meV)	$E_V + 86$	$E_V + 86$	$E_V + 86$
N_{A2} ($\times 10^{16}$ cm $^{-3}$)	9.3	8.2	7.3

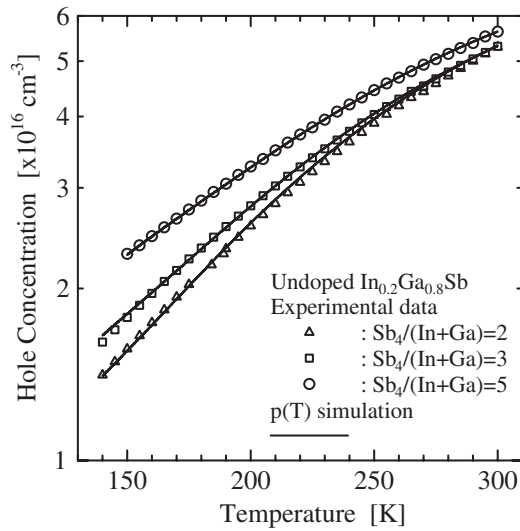


Fig. 4. Comparison of $p(T)$ simulations with experimental $p(T)$.

than Ga and In, because the vapor pressure of Sb was much higher than those of Ga and In. This suggests the formation of a vacancy at an Sb site (V_{Sb}), the substitution of Ga for Sb (Ga_{Sb}) and the substitution of In for Sb (In_{Sb}).

According to the double acceptor model,^{2,3,5,6} V_{Sb}^+ and V_{Sb}^{2+} are considered. In this case, N_{A1} should be equal to N_{A2} . Because N_{A1} increases and N_{A2} decreases with increasing BEP ratio as shown in Table I, the double acceptor model does not hold true. On the other hand, the total density of ($N_{A1} + N_{A2}$) is $\sim 1 \times 10^{17}$ cm $^{-3}$ for all the BEP ratios. Because the evaporation of Sb from the epilayer is expected to be similar for all the BEP ratios owing to the same growth temperature, two of three intrinsic defects (i.e., V_{Sb} , Ga_{Sb} , and In_{Sb}) possibly correspond to the two observed acceptor species.

In summary, it was illustrated that FCCS can determine the densities and energy levels of acceptors without any assumptions regarding acceptor species, even when the number of acceptor species included in a semiconductor is unknown. In undoped $In_{0.2}Ga_{0.8}Sb$ epilayers grown by MBE, two types of acceptor species with $E_V + 25$ meV and $E_V + 86$ meV were detected. It was found that they did not

follow the double acceptor model of V_{Sb} (i.e., V_{Sb}^+ and V_{Sb}^{2+}).

Acknowledgement

This work was partially supported by the Academic Frontier Promotion Projects of the Ministry of Education, Culture, Sports, Science and Technology (MEXT) in 1998–2002 and 2003–2008.

- 1) G. W. Turner, H. K. Choi and M. J. Manfra: Appl. Phys. Lett. **72** (1998) 876.
- 2) R. D. Baxter, R. T. Bate and F. J. Reid: J. Phys. Chem. Solids **26** (1965) 41.
- 3) R. D. Baxter, F. J. Reid and A. C. Beer: Phys. Rev. **162** (1967) 718.
- 4) M. D. Campos, A. Gouskov, L. Gouskov and J. C. Pons: J. Appl. Phys. **44** (1973) 2642.
- 5) R. A. Noack, W. Rühle and T. N. Morgan: Phys. Rev. B **18** (1978) 6944.
- 6) K. Nakashima: Jpn. J. Appl. Phys. **20** (1981) 1085.
- 7) A. H. Eltoukhy and J. E. Greene: J. Appl. Phys. **50** (1979) 6396.
- 8) P. S. Dutta, V. Prasad, H. L. Bhat and V. Kumar: J. Appl. Phys. **80** (1996) 2847.
- 9) G. Y. Zhao, H. Ebisu, T. Soga, T. Egawa, T. Jimbo and M. Umeno: Jpn. J. Appl. Phys. **37** (1998) 1704.
- 10) H. Matsuura, K. Morita, K. Nishikawa, T. Mizukoshi, M. Segawa and W. Susaki: Jpn. J. Appl. Phys. **41** (2002) 496.
- 11) H. Matsuura and K. Nishikawa: J. Appl. Phys. **97** (2005) 093711.
- 12) H. J. Hoffmann: Appl. Phys. **19** (1979) 307.
- 13) H. J. Hoffmann, H. Nakayama, T. Nishino and H. Hamakawa: Appl. Phys. A **33** (1984) 47.
- 14) H. Matsuura and K. Sonoi: Jpn. J. Appl. Phys. **35** (1996) L555.
- 15) H. Matsuura: Jpn. J. Appl. Phys. **36** (1997) 3541.
- 16) H. Matsuura, Y. Uchida, T. Hisamatsu and S. Matsuda: Jpn. J. Appl. Phys. **37** (1998) 6034.
- 17) H. Matsuura, Y. Uchida, N. Nagai, T. Hisamatsu, T. Aburaya and S. Matsuda: Appl. Phys. Lett. **76** (2000) 2092.
- 18) H. Matsuura, H. Iwata, S. Kagamihara, R. Ishihara, M. Komeda, H. Imai, M. Kikuta, Y. Inoue, T. Hisamatsu, S. Kawakita, T. Ohshima and H. Itoh: Jpn. J. Appl. Phys. **45** (2006) 2648.
- 19) H. Matsuura, T. Kimoto and H. Matsunami: Jpn. J. Appl. Phys. **38** (1999) 4013.
- 20) H. Matsuura, Y. Masuda, Y. Chen and S. Nishino: Jpn. J. Appl. Phys. **39** (2000) 5069.
- 21) H. Matsuura: New J. Phys. **4** (2002) 12.
- 22) H. Matsuura, K. Sugiyama, K. Nishikawa, T. Nagata and N. Fukunaga: J. Appl. Phys. **94** (2003) 2234.
- 23) H. Matsuura, K. Aso, S. Kagamihara, H. Iwata, T. Ishida and K. Nishikawa: Appl. Phys. Lett. **83** (2003) 4981.
- 24) H. Matsuura: J. Appl. Phys. **95** (2004) 4213.
- 25) H. Matsuura, M. Komeda, S. Kagamihara, H. Iwata, R. Ishihara, T. Hatakeyama, T. Watanabe, K. Kojima, T. Shinohe and K. Arai: J. Appl. Phys. **96** (2004) 2708.
- 26) S. Kagamihara, H. Matsuura, T. Hatakeyama, T. Watanabe, M. Kushibe, T. Shinohe and K. Arai: J. Appl. Phys. **96** (2004) 5601.
- 27) H. Matsuura, H. Nagasawa, K. Yagi and T. Kawahara: J. Appl. Phys. **96** (2004) 7346.
- 28) H. Matsuura, D. Katsuya, T. Ishida, S. Kagamihara, K. Aso, H. Iwata, T. Aki, S.-W. Kim, T. Shibata and T. Suzuki: Phys. Status Solidi C **0** (2003) 2214.